SYSTEM FOR MEASURING AIRFLOW PARAMETERS NEAR THE OCEAN SURFACE

S. I. Gabrilovich, S. A. Levchenko, and S. I. Shabunya

UDC 533.6.08

An acoustical method is described for measuring the characteristics of airflows at the boundary between the ocean and the atmosphere. Experimental results are given from measurements of the vertical component of the airflow velocity.

Investigations of the hydrodynamic characteristics of air currents in overwater atmospheric layers from on board a scientific research ship pose a complex and multifaceted problem because of the large volume of input data involved, the simultaneous use of different primary sensors, and the need to calculate a broad set of characteristics by specified algorithms.

Within the context of this problem, investigations of turbulent momentum fluxes and heat fluxes are of special interest, specifically the vertical heat flux

$$H_0 = C_p \rho \overline{U_3' \Theta'}$$

and the horizontal tangential frictional stress vector

$$\tau = i\tau_x + j\tau_y;\ \tau_x = -\rho \overline{U_3' U_1'};\ \tau_y = -\rho \overline{U_3' U_2'}.$$

We have thus reduced the problem to measurement of the fluctuation characteristics of the airflow temperature and velocity. Also, since it is required to determine the indicated correlation products, all quantities must be measured at a single point at the same time. It should be noted that when measurements are performed from on board a research ship subjected to rolling, provision must be made for the acquisition of reliable data. Rolling creates a drift velocity, changes the orientation of the anemometer coordinate system (frame) relative to the inertial frame, and causes the measurements to be performed at different points in space in correspondence with the path of the transducers. In view of the impossibility of isolating the transducers 100% from rolling, a special algorithm must be provided to distinguish useful data. A good basis for such correction of the initial data is the condition of noncorrelation between the fluctuations of the meteorological parameters and the sea-state parameters; laboratory experiments [1] have shown that this condition holds when the transducers are positioned at a height four times the wave amplitude.

According to estimates, the measurements must be performed in a volume not to exceed 0.5 × 0.5 × 0.5 m for a range of energy-carrying frequencies from 0.01 Hz to 20 Hz at a velocity of 10 m/sec; for correct data processing the sampling frequency used to measure the parameters must not be greater than 40 Hz, and the duration of the recorded samples must be at least $2 \cdot 10^3$ sec.

Four basic types of anemometers are currently used to measure wind speed and direction in micrometeorology: cup, propeller, vane, and sonic (or acoustic) anemometers. All standard observations are based on the first three types of instruments. They have the common advantages of structural simplicity, reliability, and the capability of operating within a broad range of climatic conditions. However, all mechanical anemometers have inherent shortcomings such as slow response, a strong dependence of the measurements on the angle of flow around them, nonlinearity of the dynamic parameters, and low accuracy at small flow velocities (up to 1 m/sec). Wyngaard [2] discusses the characteristics of these types of anemometers in detail.

A. V. Lykov Institute of Heat and Mass Transfer, Academy of Sciences of the Belorussian SSR, Minsk. Translated from Inzhenerno-Fizicheskii Zhurnal, Vol. 59, No. 6, pp. 1005-1011, December, 1990. Original article submitted February 13, 1989.

 0022-0841/90/5906-1602$12.50

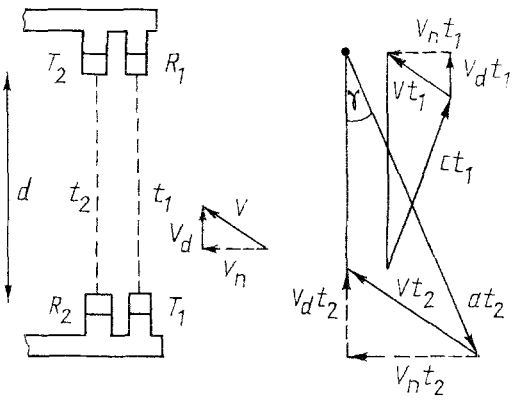

Fig. 1. Operating principle of the sonic anemometer.

We chose the acoustical measurement method to solve the stated problem. It has the advantages of fast response, the capability of operating at low velocities (for measurements of the vertical component of the velocity vector), and the fact that the velocity readings do not depend on the ambient temperature. The sonic anemometer can also be used for simultaneous measurement of the velocity of the medium and the sound velocity in the medium; the latter velocity depends on the air temperature and, to an insignificant degree, on the humidity. Complexity of data processing is inherent in this anemometer, but is not really significant, because the instrument is connected to an automated system, and all data processing is taken care of in a microcomputer.

The operating principle of the sonic anemometer [3] is based on measurement of the sound transmission time and is illustrated in Fig. 1 for a single-component instrument. Let two pairs of transducers be given: radiators T_A, T_B and receivers R_A, R_B. The wind velocity vector $\mathbf{V}$ has components V_d and V_n along and across the transducer axes. We assume that these velocities are invariant along the transmission path of the acoustic signal. The transit times t_1 and t_2 for other pulses radiated simultaneously from T_A and T_B are

$$t_1 = \frac{d}{C\cos\gamma + V_d}; \quad t_2 = \frac{d}{C\cos\gamma - V_d};$$

$$\gamma = \arcsin(V_n/C).$$

The projection of the flow velocity vector onto the axis of the sonic anemometer and the sound velocity are then equal to

$$V_d = \frac{d}{2}\left(\frac{1}{t_1} - \frac{1}{t_2}\right);$$

$$C = \frac{d}{2A}\left(\frac{1}{t_1} + \frac{1}{t_2}\right); \quad A = \sqrt{1 - \frac{V_n^2}{C^2}}.$$

If $V^2 \ll C^2$, as is certainly true for $|V| < 30$ m/sec, we have $A \approx 1$.

The frequency of the sound radiation must, on the one hand, be such as to ensure low absorption of ultrasound in the medium, i.e., it must be lower than 100 kHz; on the other hand, it must be above the frequency range of turbulent fluctuations and acoustic noise in air, i.e., it must be above 20 kHz. On the basis of these conditions the optimum radiation is ultrasound with a frequency of 40-60 kHz.

We have developed a pulsed three-component sonic anemometer with three mutually perpendicular pairs of transducers. Each channel incorporates two transducers, rather than four as in Fig. 1. Each transducer functions alternately as both receiver and radiator, and the radiators operate alternately in that capacity. This scheme eliminates crossover noise between channels. We denote the transducer pairs by A–C, B–D (horizontal), and E–F (vertical). The distance between the transducer is made equal to 0.4 m.

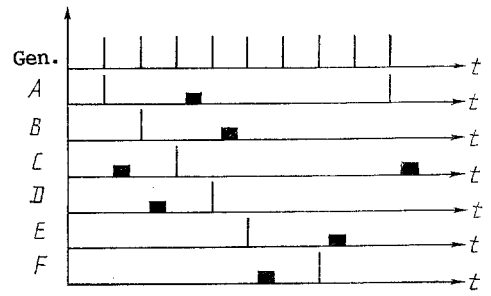

Fig. 2. Timing diagram for interaction of the transducers (the dark rectangles indicate the time intervals in which the transducer is open for reception).

The transit time of the ultrasonic pulse between transducers is approximately 1.2 msec in the absence of airflow, but this time can vary between 0.95 msec and 1.5 msec as the ambient temperature varies from 10°C to 40°C and as the flow velocity varies within the limits of ±65 m/sec. Proceeding from this fact, we set the frequency of the pulse generator equal to 400 Hz (period between pulses: 2.5 msec). To diminish the influence of noise, the receiver is not open the entire time, but only during the time in which its pulse is expected (Fig. 2). For example, if transducer B transmits in a given cycle, receiver D is open for reception in the time interval between 0.7 msec and 1.8 msec from the instant of transmission by transducer B.

The transducers are UZP-2 ultrasonic microphones which have a nominal frequency range of 31.5-50 kHz. They are capacitative transducers (capacitance 100 ± 15 pF) with a polytetraphthalate thin-film diaphragm of thickness 4 μm and a 1-μm metallized coating. The transducers are fed by a constant bias voltage of 200 V and are driven by a short negative electrical pulse of duration 5 μsec. The microphone is driven at its resonance frequency, and because of its low Q the resonance signal decays rapidly (in 5-10 periods). The transmitted pulse is received by the other transducer in the pair and is amplified by a wideband preamplifier, which is set up alongside the microphone to reduce stray capacitances and to increase the sensitivity. The received and amplified pulse is then sent to the anemometer unit (Fig. 3).

This unit is housed separately close to the transducers and executes the following functions:

reception of 400-Hz command pulses from the microcomputer;

shaping and output of driving pulses to radiators in accordance with the timing diagram (see Fig. 2);

selection of the correct receiver (Fig. 2) and opening of the circuit for transmission of the received pulse 0.7-1.8 msec after the instant of radiation;

comparison of the received signal with a preset threshold and shaping of output pulses corresponding to the instant of reception of ultrasonic radiation;

separate automatic threshold adjustment for each channel so that the noise immunity can be significantly enhanced;

shaping of an output sequence of signals and transmission of the sequence to a time-interval meter (TIM), which is interfaced with the microcomputer.

The transit times must be determined in order to find the flow and sound velocities in the medium. Two alternatives are possible here: 1) measurement of the transit times in the anemometer and transfer of the digitally coded results to a computer; 2) transfer of the signals into an automated system with subsequent measurement in the system itself. The second alternative was found to be more practical.

The transit time is measured with a resolution of $2 \cdot 10^{-7}$ sec, which corresponds to a resolution of $3 \cdot 10^{-3}$ m/sec in the measured flow and sound velocities. For a more precise determination of the transit time in the TIM, first the time between leading edges of the initial and final pulses is measured, then the duration of the final pulse is measured, and half of this time is added to the result. This procedure makes it possible to fix the transit time interval from the extremum of the received pulse and to eliminate any dependence on the level of the threshold set in the sonic anemometer (Fig. 4).

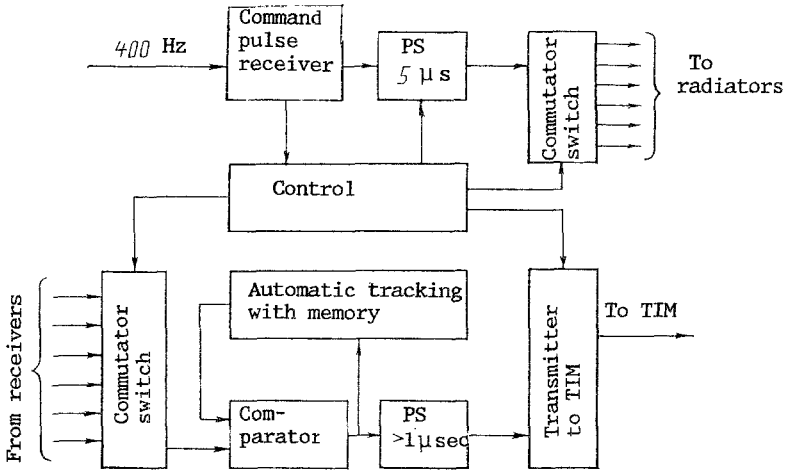

Fig. 3. Simplified block diagram of the sonic anemometer (the transducers and preamplifiers are not shown). PS) Pulse shaper; TIM) time-interval meter.

We now consider the influence of various factors on the error of measurement of the flow velocity. The temperature and humidity change the sound velocity appreciably, but these factors can be disregarded in measurement of the flow velocity. As mentioned earlier [1], the most serious and by no means trivial problem is the distortion of the flow by insertion of the meter itself. The anemometer is designed as a horizontally symmetrical structure, and the microphones together with the preamplifiers are enclosed in streamlined ellipsoidal casings. Nonetheless, the existence of velocity defects in the turbulent wakes of the streamlined transducers induces systematic errors, i.e., the reading of the average flow velocity is understated relative to the true value. These errors must be taken into account during calibration. The anemometer characteristics have been determined in a wind tunnel in the velocity range 2-50 m/sec. It was found that the following correction factor must be introduced for longitudinal flow around the given structure:

$$K_1 = U_{\text{tru}}/U_{\text{msr}} = 1.369 \pm 0.015.$$

The measured modulus of the velocity obtained from two mutually perpendicular pairs of transducers was also determined as a function of the flow impingence angle. The recorded calibration curve for rotation of the meter in the horizontal plane (with points recorded every 10°) was then approximated according to the least-squares method by a functional relation of the form

$$K_2 = 0.127 \sin^2 2\varphi + 1.061.$$

The error after correction is 3%.

The angle determined as $\tan^{-1}(U_x/U_y)$ also deviated from the true value. Although this deviation is not greater than ±3°, the dependence of the true angle on the measured angle was still approximated by the empirical formula

$$\alpha = \varphi - 2.5 \sin 4\varphi + 0.4.$$

This correction helped to reduce the angle measurement error to ±1°.

The anemometer demonstrated high efficiency in the range of velocities 2-22 m/sec. At higher flow velocities the velocity head exerts static pressure on the diaphragm of the transmitting microphone, sharply attenuating the ultrasonic radiation.

As for operation at low flow velocities (down to 0), the linear response of the sonic anemometer precludes the possibility of additional error sources. Based on its operating principle alone, this anemometer should operate quite well at low velocities. However, it could not be calibrated under laboratory conditions, because the operation of the wind tunnel is unstable at low velocities, and the measurement of such velocities is not sufficiently accurate. Consequently, the shipboard readings of the sonic anemometer were further checked against those of an MS-13 manual cup anemometer in the velocity interval

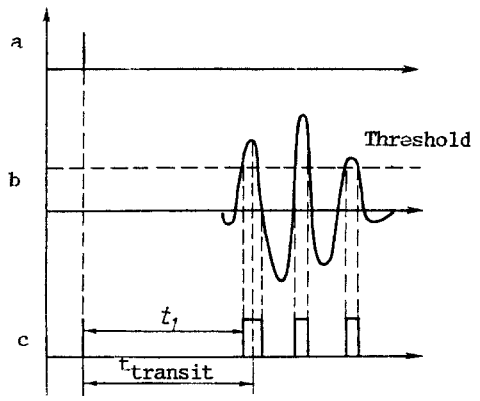

Fig. 4. Transit-time measurement. a) Radiated pulse; b) received pulse; c) output pulse train sent to the time-interval meter after the sonic anemometer.

1-2 m/sec. The discrepancy in the readings did not exceed 0.18 m/sec, which falls within the error limits of both instruments.

An automated data acquisition and processing system incorporating an Élektronika NMS 11100.1 microcomputer was used for the investigations. The system ensures operation with a series of primary instruments, including the ultrasonic anemometer. Moreover, measurements from on board the research ship require data on the spatial orientation of the anemometer relative to the horizon. A gyroscopic angle-measuring instrument utilizing an AGB-3K gyrohorizon was connected to the system for this purpose.

The above-described measurement system was used to determine the temperature and velocity fields of air currents in the tropical zone of the Pacific Ocean. An ultrasonic anemometer was mounted on an actinometer arm at a distance of 6 m from the bow section of the ship's hull. We shall give only some representative results here. (More detailed information about the results and the processing procedure will be published later.)

In most of the experiments the results pertaining to the velocity field were consistent with standard estimates [4]. In the course of processing the measurements, however, the most interesting results were the average values obtained for the vertical component of the airflow velocity on a test range in the South China Sea. These averages fell within the interval 0.5-1.1 m/sec. Such large values stimulated considerable interest and motivated a careful analysis of the causes of possible errors, both instrumental and methodological. The analysis showed that only two factors could produce large errors: flow around the hull of the ship and tilting of the transducer relative to the vertical. We therefore conducted special methodological experiments. In one of them we measured the vertical velocity for a fixed orientation of the transducer, both in drift with the wind blowing at a 110° angle relative to the ship's axis and again with the ship moving against the wind. In the second experiment, for a fixed orientation of the transducer, the ship rotated about its own axis, facing in all directions relative to the wind.

These experiments elicited large variations of the recorded airflow parameters, but this mainly affected the horizontal component of the velocity with the wind blowing astern.

The average value of the vertical component also varied, but kept the same sign and fell within the interval 0.5-1.1 m/sec.

The above-described system demonstrated the efficiency and feasibility of obtaining reliable information in measurements from on board a research ship on a rolling sea. The reported values of the vertical velocity component require close attention and further study.

NOTATION

C_p, heat capacity of air at constant pressure; ρ, density; U'_1, U'_2, U'_3, fluctuations of the two horizontal components and the vertical component of the airflow velocity vector; Θ', temperature fluctuations; d, acoustic path length; C, sound velocity in air; U_{tru}, true flow velocity; U_{msr}, measured flow velocity; φ, measured angle relative to one of the orthogonal axes of the instrument in the horizontal plane; U_x, U_y, measured orthogonal components; α, true angle.

LITERATURE CITED

1. J. M. Kendall, J. Fluid Mech., 41, 2 (1970).
2. J. C. Wyngaard, Annual Review of Fluid Mechanics, Vol. 13, Annual Reviews, Palo Alto, Calif. (1981), pp. 399-423.
3. W. Frost and T. H. Moulden (eds.), Handbook of Turbulence: Fundamentals and Applications, Plenum Press, New York–London (1977).
4. A. S. Monin and R. V. Ozmidov, Ocean Turbulence [in Russian], Leningrad (1981).

DERIVATION OF INITIAL STATES IN INVESTIGATION OF NUCLEATION BY THE THERMODIFFUSION-CHAMBER METHOD

V. T. Borukhov, N. V. Pavlyukevich, I. Smolik, and S. P. Fisenko

UDC 536.42

A method of deriving the dimensions and coordinates of new-phase nuclei (initial states) in investigating nucleation in spatially inhomogeneous systems is developed. The results of analyzing experimental data taking account of the possible influence of Brownian motion on the nucleation kinetics are given.

To study volume condensation (nucleation), thermodiffusional chambers are in increasing use. The basic aim of experimental investigations in this area is to find the dependence of the nucleation rate I on the degree of supersaturation S with a known temperature of the vapor–gas mixture. Unambiguous interpretation of the experimental results is difficult, however, because of two factors: first, the region of maximum supersaturation within which nuclei of new phase are formed is of finite size; second, the optical methods of recording new-phase particles used in the experimental investigations permit the recording of particles which are of the order of a micron in size, whereas the critical nuclei of new phase are of size $R \sim 10^{-9}$ m.

In connection with this, a method of deriving the initial states using experimental data on the parameters of the new-phase particles [3] is developed here on the basis of a mathematical model of the growth and motion of the new-phase particles forming in the thermodiffusional chamber [1, 2].

As shown by experiments, the interpretation of experimental data on the nucleation of vapor in the thermodiffusion chamber may be divided into three stages. These stages, which differ both in the depth of analysis and in the volume of experimental data required, will be described in sequence. The simplest is the first, in which minimal experimental data is required.

Stage 1 (Phenomenological)

Suppose that there is experimental information that new-phase nuclei form in the chamber with temperatures of the lower and upper plates T_1 and T_2 and ballast-gas pressure P and are able to grow, in these conditions, to dimensions permitting recording by optical methods. In this case, as shown in [2], it is necessary to plot graphs of the dimensionless quantity $\Delta\Phi(g^*(z))/kT(z)$, where $\Delta\Phi(g^*(z))$ is the work of critical-nucleus formation in conditions corresponding to the coordinate z.

Note that in the present work all the notation is analogous to that in [2]. In Fig. 1, the graph of the dimensionless work of critical-nuclei formation of dioctylphthalate

A. V. Lykov Institute of Heat and Mass Transfer, Academy of Sciences of the Belorussian SSR, Minsk. Institute of Theoretical Principles of Chemical Processes, Prague.
Translated from Inzhenerno-Fizicheskii Zhurnal, Vol. 59, No. 6, pp. 1011-1016, December, 1990. Original article submitted November 27, 1989.

0022-0841/90/5906-1607$12.50